Composite Structures 143 (2016) 93–102

Contents lists available at ScienceDirect

Composite Structures

journal homepage: www.elsevier.com/locate/compstruct

Aeroelastic characteristics of magneto-rheological fluid sandwich beams in supersonic airflow

Mojtaba Asgari, Mohammad Ali Kouchakzadeh *

Department of Aerospace Engineering, Sharif University of Technology, Azadi Street, P.O. Box 11155-8639, Tehran, Iran

ARTICLE INFO

Article history:
Available online 9 February 2016

Keywords:
Sandwich beam
Magneto-rheological fluid
Supersonic flow
Flutter

ABSTRACT

Supersonic aeroelastic instability of a three-layered sandwich beam of rectangular cross section with an adaptive magneto-rheological fluid (MRF) core layer is investigated. The panel is excited by an airflow along it's longitudinal direction. The problem formulation is based on classical beam theory for the face layers, magnetic field dependent complex modulus approach for viscoelastic material model and the linear first-order piston theory for aerodynamic pressure. The classical Hamilton's principle and the assumed mode method are used to set up the equations of motion. The validity of the derived formulation is confirmed through comparison with the available results in the literature. The effects of applied magnetic field, core layer thickness and constraining layer thickness on the critical aerodynamic pressure are studied. The onset of instability in terms of the critical value of the nondimensional aerodynamic pressure for the sandwich beam is calculated using the p-method scheme. Simply supported, clamped–clamped and clamped-free boundary conditions are considered. The results show that the magnetic field intensity and thickness ratios have significant effects on the instability bounds.

1. Introduction

Thin walled structural components exposed to high velocity airflow on the outer surface of aerospace vehicle may become unstable at a certain critical aerodynamic pressure. At this pressure the motion of the surface panels grows with time until the in-plane tensile stresses induced by the geometric nonlinearities restrain the vibration amplitude of the structure. This phenomena, is known as panel flutter and may occur frequently under transonic, supersonic or hypersonic environments as a result of interactions between the inertial force, elastic force and the aerodynamic loads induced by the airflow [1–3]. Oscillatory nature of the flutter can cause high stresses and result in the fatigue of thin walled components or supporting structures, excessive noise levels in vehicle compartments near the fluttering panel or functional failure of the equipment attached to the structure.

Since the panel flutter phenomenon first occurred on the early V-2 rockets, a large number of failures have been caused by the aeroelastic and aerothermoelastic flutters in the history of aerospace development [4,5]. In order to reduce the possibility of catastrophic flight accidents caused by flutter, it is necessary to control and suppress the fluttering structure/components of an aerospace vehicle.

In order to improve the aeroelastic instability characteristics of an aerospace structure, one should manage to increase the instability bound by changing the structural complex eigenvalues. It is well known that the structural eigenvalues are related to the structural stiffness, damping and mass matrices. By changing the structural stiffness, damping and mass properties, the flutter characteristics of the structure may be possibly improved.

Adaptive structures are structures which can adopt, evolve or change their properties or behavior in response to the environment around them due to the incorporation of a controllable component such as piezoelectric [6], shape memory alloy (SMA) [7], electro-rheological (ER) [8] and magneto-rheological (MR) materials [9].

The stiffness and damping characteristics of adaptive structures comprising magneto and electro-rheological fluids can rapidly and reversibly be changed by application of external magnetic/electric field. Nowadays, these structures are being used increasingly in vibration and noise control [10–14]. These structures have other valuable advantages such as low energy loss, simplicity, robustness and easy controllability.

Constrained layer damping (CLD) is an effective approach for improving the dynamic behavior of flexible structures which is used mostly in aerospace and automotive engineering. Traditionally, viscoelastic materials are used in this approach to suppress

* Corresponding author. Tel.: +98 21 66164641; fax: +98 21 66022731.
E-mail address: mak@sharif.edu (M.A. Kouchakzadeh).

http://dx.doi.org/10.1016/j.compstruct.2016.02.015
0263-8223/

excessive vibration, however due to fixed damping and stiffness properties of the usual viscoelastic materials, the vibration control performance of these structures is limited to a narrow frequency range. Recently, MR/ER materials have been utilized as a core in sandwich structure which leads to distributed stiffness and damping properties of the structure and facilitates vibration control over a broad range of frequencies. For the first time Gandhi et al. [15] experimentally analyzed application of ER materials as a core in a cantilevered sandwich beam and concluded that the structure damping ratio and natural frequencies increase with increase in electric filed. Another experimental investigation on a cantilevered beam locally linked by an electro-rheological fluid layer to ground was conducted by Haiqing et al. [16]. In this research the ER fluid layer was locally applied to the beam as a complex spring and it was found that the frequency response function curve of the beam changed drastically under electric field. It is also reported that the vibration characteristics of the cantilevered beam with locally applied ER fluid layer treatment is more sensitive to the electric field than a sandwich beam. Using Mead and Markus sandwich beam model [17], vibration characteristics of viscoelastically damped sandwich ER beam was calculated for clamped-free and clamped–clamped boundary conditions by Yalcintas and Coulter [18]. Hasheminajad and Maleki [8], studied the free and steady state forced vibration characteristics of a sandwich plate with ER fluid core and cross-ply elastic composite laminate face layers using Hamilton's principles and Navier technique under simply supported boundary conditions for various electric field strength, geometric aspect ratio and ER core layer thicknesses. They concluded that the natural frequency increases monotonically with increasing electric field strength but loss factor of the structure increases to its maximum value and decreases with further increase in the field intensity. Furthermore, the natural frequencies increase with increasing geometric aspect ratio and decrease with increasing ER core layer thickness. Allahverdizade and his coworkers conducted a series of analytical and experimental studies on linear and nonlinear vibration behavior of functionally graded ER sandwich beams [19–22].

Compared to the works on structures embedded with ER fluids, limited results are available on MR based sandwich structures. First investigation on the use of MR fluid in sandwich structures conducted by Yalcintas and Dai [23]. They compared effectiveness of using MR and ER fluids in adaptive structures and concluded that by using MR materials as a core, the natural frequencies of the structure increases almost two times compared with ER counterpart. The controllable capabilities of an MR sandwich beam have been investigated theoretically and experimentally by Sun et al. [24]. They used oscillatory rheometry technique to derive the relationship between the magnetic field intensity and complex shear modulus of MR materials. Yeh and Shih [25] determined the regions of dynamic stability and dynamic response of an MR simply supported sandwich beam subjected to the axial harmonic load using incremental harmonic balance (IHB) method. Kumar and Ganesan [26] used finite element formulation to study the effects of core thickness, electric voltage and magnetic field on the vibration and damping behavior of the clamped free hollow sandwich box column containing a viscoelastic, electro-rheological or magneto-rheological fluid core. Rajamohan et al. [27] used finite element method and Ritz formulation to study the vibration characteristics of a sandwich beam with MR fluid core with various boundary conditions. They also validated their formulations through experimental study on a cantilevered sandwich beam. In addition, they estimated complex shear modulus of the MR fluid based on the single-degree-of-freedom (SDOF) vibration behavior according to the procedure proposed by Choi et al. [28]. They concluded that increasing the magnetic field intensity increases natural frequencies for all modes and loss factor at higher modes. It has been observed that simply supported boundary condition has the highest loss factor at lower modes and clamped-free one at higher modes. Furthermore, it is observed that by increasing the thickness of the MR layer, natural frequencies at all modes decreases while the loss factor increases at the first two modes. Rajamohan et al. [29] investigated the influence of length and location of the MR fluid layer segment under different magnetic field intensities in the dynamic characteristics of a partially treated MR fluid beam for different boundary conditions and compared the results with the fully treated counterpart. It is observed, in addition to the intensity of the applied magnetic field and boundary conditions, the location and length of the fluid pocket strongly affects the natural frequencies and transverse displacement response of the partially treated MR beam. Optimal locations for the MR fluid treatment in partially filled MR sandwich beam to individually and simultaneously attain to maximum modal damping related to the first five flexural vibration mode of the beam is obtained by Rajamohan et al. [30] using genetic algorithm and sequential quadratic programming algorithm. Semi active optimal vibration control of fully and partially treated clamped-free MR sandwich beam conducted using linear quadratic regulator (LQR) optimal control strategy by Rajamohan et al. [12]. The results suggested about 85% reduction in the free vibration settling time and 25% reduction in the tip deflection. Ndemanou et al. [31] carried out a study on vibration suppression of a cantilevered Timoshenko beam subjected to the earthquake load by a magneto-rheological damper localized at a specific point of the beam. Ramamoorthy et al. [10] numerically and experimentally analyzed free and forced vibration behavior of a partially treated laminated composite MR fluid sandwich plate. The study concluded more pronounced effect of using MR fluid segment in partial region of large components on vibration amplitude reduction and decreasing the magnitude of the peak response at all vibration modes with increase in magnetic field intensity. Manoharan et al. [11] investigated the effect of magnetic field intensity, thickness of MR fluid layer and the ply orientation of the composite face layers on the natural frequencies and loss factors of a laminated composite MR fluid sandwich rectangular plate using finite element formulation. In a recent numerical and experimental study, Eshaghi et al. [32] analyzed the effect of variation in the magnetic flux, core layer thickness and plate aspect ratio on the vibration behavior of an MR sandwich plate.

Many research works have been carried out on vibrating and damping behavior of MR/ER sandwich adaptive structures; however, a limited number of analyses are available on aeroelastic behavior of MR/ER based adaptive structures. The first study on the flutter suppression capability of ER sandwich beams was conducted by Hasheminejad et al. [33]. They used sliding mode control algorithm to suppress the supersonic flutter instability of a simply supported sandwich beam coupled to an elastic foundation. Supersonic flutter analysis of a sandwich ER rectangular plate with orthotropic face layers was conducted by Rahiminasab and Rezaeepazhand [34]. Various parametric studies were performed in terms of variations of the critical aerodynamic pressure as functions of the applied electric field, thickness of the ER fluid layer, electro-rheological fluid type, constraining layer thickness and fiber angle of orthotropic faces for simply supported and fully clamped boundary conditions. Hasheminajad and his coworkers [35–37] further investigated supersonic panel flutter semi active control of ER based rectangular sandwich plates and cylindrical shell using sliding mode control method and Rung-Kutta time integration algorithm.

To the author's knowledge, no report is available on the aeroelastic behavior of MR sandwich structures under supersonic flow. A few studies on the aeroelastic behavior of ER based adaptive structures are available [33–36]. These are limited to flutter control of a specific structure with inadequate parametric investigation on the

effect of core and constraining layers thicknesses. Rigorous investigations involving the effect of various parameters such as boundary conditions, constraining and core layer thicknesses, and magnetic field strength on the instability boundary seem to be required. The main objective of this paper is to fill such a gap. In this study, the Hamilton's principle along with the assumed mode method is adopted to obtain the aeroelastic characteristics of the sandwich beam. The classical beam theory is used for structural modeling of the face layers. Simply supported (S-S), clamped–clamped (C–C) and clamped-free (C-F) boundary conditions are taken into account. Effect of magnetic field strength, MR fluid layer thickness, and constraining layer thickness on non-dimensional aerodynamic pressure of the sandwich adaptive beam is investigated.

2. Mathematical modeling

Consider a three layer sandwich beam with magneto-rheological fluid core of length L, width b and thickness h which is subjected to a supersonic flow as shown in Fig. 1. The beam is composed of an elastic base layer of thickness h_b, a constraining elastic layer of thickness h_c and a MR fluid core of thickness h_f.

Simplification is an integral part of any mathematical modeling. Here, some simplifications are considered to make the model of the problem. Since Young's modulus of the MR fluid is almost negligible compared to that of the elastic layers, one can neglect normal stress in the core. In addition, it is assumed that the fluid layer thickness is very small compared to its length and no slip occurs at the interface between the face layers and the MR layer. The thicknesses of elastic layers are very small compared to the length of the beam and one can neglect the shear strain in these layers. Furthermore, all of the layers experience the same transverse displacement.

With the above-mentioned assumptions, the total displacement components of the upper and lower elastic layers at a material point (x, z_i) can be expressed as [38]:

$$u^b(x,z_b,t) = u_b(x,t) - z_b\frac{\partial w}{\partial x}(x,t) \tag{1}$$

$$u^c(x,z_c,t) = u_c(x,t) - z_c\frac{\partial w}{\partial x}(x,t) \tag{2}$$

$$w^b(x,z_b,t) = w^c(x,z_c,t) = w(x,t) \tag{3}$$

where u_b and u_c are the mid-plane displacements in the x direction, w denotes the transverse displacement of the layers, z_b, z_c are the local transverse coordinates of the two face layers, and t is the time.

Using the linear strain-displacement relations, the strain components in the elastic layers can be written as [38]:

$$\epsilon_x^b = \frac{\partial u_b}{\partial x} - z_b\frac{\partial^2 w}{\partial x^2} \tag{4}$$

$$\epsilon_x^c = \frac{\partial u_c}{\partial x} - z_c\frac{\partial^2 w}{\partial x^2} \tag{5}$$

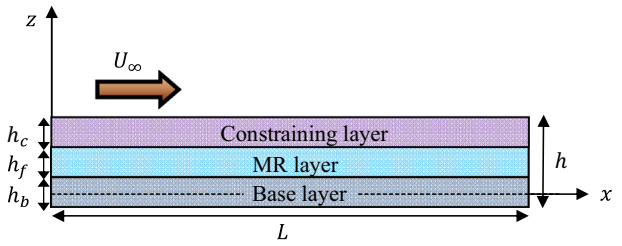

Fig. 1. Geometry of sandwich beam with width b.

In addition, the normal stress components within the base and constraining layers are obtained from Hook's law as

$$\sigma_x^b = E_b\epsilon_x^b = E_b\left(\frac{\partial u_b}{\partial x} - z_b\frac{\partial^2 w}{\partial x^2}\right) \tag{6}$$

$$\sigma_x^c = E_c\epsilon_x^c = E_c\left(\frac{\partial u_c}{\partial x} - z_c\frac{\partial^2 w}{\partial x^2}\right) \tag{7}$$

Displacement field of the core is expressed as

$$u^f(x,z_f,t) = -z_f\varphi(x,t) \tag{8}$$

By using the displacements continuity on the upper and lower interface of the sandwich beam, one can obtain φ as follow:

$$\varphi = \frac{u_b - u_c}{h_f} - \frac{h_b + h_c}{2h_f}\frac{\partial w}{\partial x} \tag{9}$$

Thus, the shear strain of the MR core is obtained as

$$\gamma = \gamma_{xz} = \frac{\partial w^f}{\partial x} + \frac{\partial u^f}{\partial z_f} = \frac{\partial w}{\partial x} - \varphi = \frac{D}{h_f}\frac{\partial w}{\partial x} + \frac{u_c - u_b}{h_f} \tag{10}$$

where $D = h_f + (h_b + h_c)/2$.

Longitudinal forces in each of the elastic layers which is denoted by F_c and F_b with their lines of action in the midplanes of the elastic layers are related to the longitudinal displacements by

$$F_c = E_cA_c\frac{\partial u_c}{\partial x}, \quad F_b = E_bA_b\frac{\partial u_b}{\partial x} \tag{11}$$

where A_b and A_c are the cross-section areas of the base and constraining layers, respectively and E_b and E_c are the corresponding Young's moduli.

Neglecting in-plane inertia of the base and constraining layers, since the beam is assumed to be free of longitudinal forces, F_b and F_c must be equal in magnitude and opposite in direction, i.e., $F_c = -F_b$:

$$E_cA_c\frac{\partial u_c}{\partial x} = -E_bA_b\frac{\partial u_b}{\partial x} \tag{12}$$

Integrating the above equation with respect to x, results in

$$u_c = -eu_b \tag{13}$$

where $e = E_bA_b/E_cA_c$.

The shear stress-strain properties of magneto-rheological material strongly depend upon the applied magnetic field [39,40] and can be divided in two distinguished regions, referred to as 'pre-yield' and 'post-yield' regions, as shown in Fig. 2.

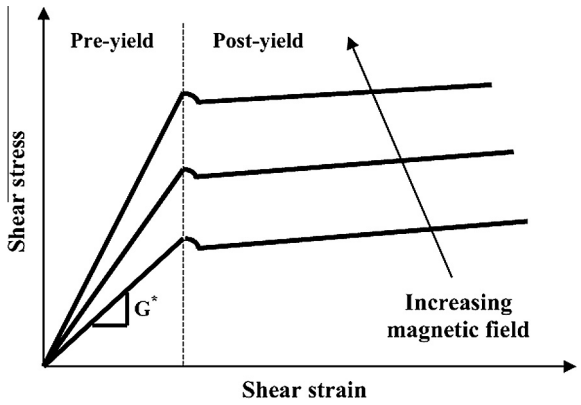

Fig. 2. Shear stress-shear strain relationship of MR material.

In the pre-yield region (at strains of order 10^{-3}) the MR fluid exhibits linear viscoelastic behavior [39], which has been described by the field dependent complex modulus as

$$G^*(\mathrm{B}) = G'(\mathrm{B}) + \mathrm{i}G''(\mathrm{B}) = G'(\mathrm{B})(1 + \mathrm{i}\eta(\mathrm{B})) \tag{14}$$

where the storage modulus G' and loss modulus G'' are proportional to the averaged energy stored and dissipated over a cycle of deformation per unit volume of the MR material respectively. Moreover, η represents the material loss factor which is a measure of the ratio of the energy dissipated from the material per radian to the stored energy during the steady state sinusoidal excitation.

2.1. Governing equation of motion

General form of the Hamilton's principle is used to determine the equation of motion along with the associated edge boundary conditions of the MR sandwich beam. It can be written as [41]

$$\int_{t_1}^{t_2} \delta(U - T + W_{\mathrm{nc}})dt = 0 \tag{15}$$

where δ denotes the first variation, T and U are the kinetic and potential energy of the total system, W_{nc} is the work done by the non-conservative forces, and t_1 and t_2 are the integration time limits.

The total kinetic energy of the system (T) comprises those associated with the transverse motion of the elastic face layers and the MR layer (T_1) and the rotational deformation of the MR core (T_2) expressed as:

$$T_1 = \frac{1}{2}\int_0^L (\rho_b A_b + \rho_f A_f + \rho_c A_c)\left(\frac{\partial w}{\partial t}\right)^2 dx \tag{16}$$

$$T_2 = \frac{1}{2}\int_0^L \rho_f I_f \left[\frac{D}{h_f}\frac{\partial^2 w}{\partial x \partial t} - \frac{(1+e)}{h_f}\frac{\partial u}{\partial t}\right]^2 dx \tag{17}$$

$$T = T_1 + T_2 \tag{18}$$

where I_f is the second moment of inertia of the MR layer and ρ_b and ρ_c are the mass densities of the base and constraining layers respectively. Hereafter, we use u instead of u_b in our formulations.

The strain energy of the elastic face layers due to axial deformations (U_1) and the one due to transverse deformations (U_2) may be expressed as

$$U_1 = \frac{1}{2}\int_0^L (E_b A_b + E_c A_c e^2)\left(\frac{\partial u}{\partial x}\right)^2 dx \tag{19}$$

$$U_2 = \frac{1}{2}\int_0^L (E_c I_c + E_b I_b)\left(\frac{\partial^2 w}{\partial x^2}\right)^2 dx \tag{20}$$

where I_b and I_c are the second moments of inertia of the base and constraining layers respectively. The strain energy of the MR core can be express as

$$U_3 = \frac{1}{2}\int_0^L GA_f \left[\frac{D}{h_f}\frac{\partial w}{\partial x} - \frac{(1+e)}{h_f}u\right]^2 dx \tag{21}$$

The total strain energy (U) of the sandwich beam can be obtained by the sum of those due to elastic and MR layers as

$$U = U_1 + U_2 + U_3 \tag{22}$$

The virtual work done by the non-conservative aerodynamic pressure loading can be obtained as

$$\delta W_{\mathrm{nc}} = \int_A \Delta p\ \delta w\ dA \tag{23}$$

where A is the surface area of the upper surface of the beam which is subjected to the supersonic air flow and δp is the aerodynamic pressure load which can be described according to the linear first-order piston theory as follows [1,3]

$$\Delta p = -\zeta\frac{\partial w}{\partial x} - \mu\frac{\partial w}{\partial t} \tag{24}$$

where $\zeta = \rho_\infty U_\infty^2 \Big/ \sqrt{M_\infty^2 - 1}$ and $\mu = \rho_\infty U_\infty (M_\infty^2 - 2)/(M_\infty^2 - 1)^{3/2}$ are the aerodynamic pressure and damping parameters respectively, wherein U_∞, M_∞ and ρ_∞ are the free stream velocity, Mach number and air density. Aerodynamic damping term always stabilizes the flutter instability [42,43]. Furthermore, the interest is on the pure effect of MR layer damping on the aeroelastic characteristics of the MR sandwich beam, thus the contribution of the aerodynamic damping in the calculations may be neglected.

Using Eqs. (19) and (20) along with Eq. (18) the first variation of the kinetic energy after time integration by parts, yields

$$\begin{aligned}\int_{t_1}^{t_2} \delta T\, dt = \int_{t_1}^{t_2} \delta(T_1 + T_2)\, dt = -\int_{t_1}^{t_2}\int_0^L (&\beta_1 \ddot{w}\delta w + \beta_2 \ddot{w}'\delta w' \\ &+ \beta_3 \ddot{u}\delta w' + (\beta_3 \ddot{w}' + \beta_4 \ddot{u})\delta u)dx\, dt\end{aligned} \tag{25}$$

where β_1, β_2, β_3 and β_4 are defined as follows

$$\begin{aligned}&\beta_1 = (\rho_b A_b + \rho_f A_f + \rho_c A_c) \quad \beta_2 = \rho_f I_f \left(\frac{D}{h_f}\right)^2 \\ &\beta_3 = -\rho_f I_f \frac{(1+e)D}{h_f^2} \quad \beta_4 = \rho_f I_f \left(\frac{1+e}{h_f}\right)^2\end{aligned} \tag{26}$$

Using Eqs. (19) through (22), the strain energy of the system can be written as

$$\begin{aligned}\int_{t_1}^{t_2} \delta U\, dt &= \int_{t_1}^{t_2} \delta(U_1 + U_2 + U_3)\, dt \\ &= \int_{t_1}^{t_2}\int_0^L (\alpha_1 u'\delta u' + \alpha_2 w''\delta w'' \\ &\quad + (\alpha_3 w' + \alpha_4 u)\delta w' + (\alpha_4 w' + \alpha_5 u)\delta u)dx\, dt\end{aligned} \tag{27}$$

where

$$\begin{aligned}&\alpha_1 = E_b A_b + E_c A_c e^2 \quad \alpha_2 = E_c I_c + E_b I_b \quad \alpha_3 = GA_f \left(\frac{D}{h_f}\right)^2 \\ &\alpha_4 = -GA_f \frac{D(1+e)}{h_f^2} \quad \alpha_5 = GA_f \left(\frac{1+e}{h_f}\right)^2\end{aligned} \tag{28}$$

Aerodynamic pressure loading is

$$\int_{t_1}^{t_2} \delta W_{nc} dt = \int_{t_1}^{t_2}\int_0^L b\ \Delta p\ \delta w\ dx\ dt = -\zeta b \int_{t_1}^{t_2}\int_0^L w'\delta w\ dx\ dt \tag{29}$$

According to extended Hamilton's principle, by substituting Eqs. (25), (27) and (29) into Eq. (15), one can obtain the governing equation of motion as

$$\begin{aligned}\int_0^L (&\alpha_2 w''\delta w'' + (\alpha_3 w' + \alpha_4 u)\delta w' - \zeta b w'\delta w + \beta_1 \ddot{w}\delta w \\ &+ \beta_2 \ddot{w}'\delta w' + \beta_3 \ddot{u}\delta w')dx = 0\end{aligned} \tag{30}$$

for transverse vibration and

$$\int_0^L (\alpha_1 u'\delta u' + (\alpha_4 w' + \alpha_5 u)\delta u + (\beta_3 \ddot{w}' + \beta_4 \ddot{u})\delta u)dx = 0 \tag{31}$$

for longitudinal vibration of the MR sandwich beam.

2.2. Solution procedure

Assumed mode method is used to solve the coupled Eqs. (30) and (31) using the following relationships for transverse and longitudinal displacements

$$w(x,t)=\sum_{i=1}^{N_w}\xi_i(x)\eta_i(t) \tag{32}$$

$$u(x,t)=\sum_{i=1}^{N_u}\varphi_i(x)\delta_i(t) \tag{33}$$

where N_w and N_u are number of modes used in the transverse and longitudinal directions respectively. Also, $\xi_i(x)$ and $\varphi_i(x)$ are the transverse and longitudinal principle vibration mode shapes respectively, and $\eta_i(t)$ and $\delta_i(t)$ are the generalized coordinates of the structural system. By substituting $\xi_i(x)$ and $\varphi_i(x)$ in Eqs. (30) and (31) as admissible variations of the bending (δw) and extension (δu) of the sandwich beam and after doing some manipulations, one can obtain

$$\mathbf{M}\ddot{\mathbf{q}}+\mathbf{K}\mathbf{q}=\mathbf{0} \tag{34}$$

In the above equation $\mathbf{q}=[\xi_1\cdots\xi_{N_w},\delta_1\cdots\delta_{N_u}]$ is the vector of generalized coordinates and $\mathbf{M}$ and $\mathbf{K}$ are the structural mass and stiffness matrices, respectively which are defined as

$$\mathbf{M}=\begin{bmatrix}\mathbf{M}_{11} & \mathbf{M}_{12}\\ \mathbf{M}_{21} & \mathbf{M}_{22}\end{bmatrix},\quad \mathbf{K}=\begin{bmatrix}\mathbf{K}_{11} & \mathbf{K}_{12}\\ \mathbf{K}_{21} & \mathbf{K}_{22}\end{bmatrix} \tag{35}$$

where

$$\begin{aligned}
\mathbf{M}_{11}&=\beta_1\int_0^L\xi_i\xi_j\,dx+\beta_2\int_0^L\xi_i'\xi_j'\,dx\\
\mathbf{M}_{12}&=\beta_3\int_0^L\xi_i'\varphi_j\,dx\\
\mathbf{M}_{21}&=\beta_3\int_0^L\varphi_i\xi_j'\,dx\\
\mathbf{M}_{22}&=\beta_4\int_0^L\varphi_i\varphi_j\,dx\\
\mathbf{K}_{11}&=\alpha_2\int_0^L\xi_i''\xi_j''\,dx+\alpha_3\int_0^L\xi_i'\xi_j'\,dx-\lambda\frac{E_bI_b}{L^3}\int_0^L\xi_i'\xi_j\,dx\\
\mathbf{K}_{12}&=\alpha_4\int_0^L\xi_i'\varphi_j\,dx\\
\mathbf{K}_{21}&=\alpha_4\int_0^L\varphi_i\xi_j'\,dx\\
\mathbf{K}_{22}&=\alpha_1\int_0^L\varphi_i'\varphi_i'\,dx+\alpha_5\int_0^L\varphi_i\varphi_j\,dx
\end{aligned} \tag{36}$$

Assuming harmonic motion, $\mathbf{q}=\bar{\mathbf{q}}\exp(\mathrm{i}\delta t)$, where $\mathrm{i}=\sqrt{-1}$ and $\bar{\mathbf{q}}$ and δ are the eigenvectors and eigenvalues of the system, the discretized form of the equation of motion (Eq. (34)) is transformed into an eigenvalue problem

$$(\mathbf{M}^{-1}\mathbf{K})\bar{\mathbf{q}}=\delta^2\bar{\mathbf{q}} \tag{37}$$

Consequently, the natural frequency ω and modal loss factor η of the three layer sandwich beam can be obtained as follows:

$$\omega=\sqrt{\mathrm{Re}(\delta^2)} \tag{38}$$

$$\eta=\frac{\mathrm{Im}(\delta^2)}{\mathrm{Re}(\delta^2)} \tag{39}$$

The non-dimensional aerodynamic pressure, λ, is normally used to obtain the flutter boundary [33,44]. Here, the non-dimensional aerodynamic pressure can be defined as

$$\lambda=\zeta b\frac{L^3}{E_bI_b}=\frac{\rho_\infty U_\infty^2}{\sqrt{M_\infty^2-1}}\frac{bL^3}{E_bI_b} \tag{40}$$

By plotting loss factor for different non-dimensional aerodynamic pressures one can obtain the instability boundary. The instability will be reached when the loss factor changes from positive to negative.

In order to calculate the critical non-dimensional aerodynamic pressure (λ_{cr}), the mode shapes for the longitudinal and transverse vibration of the pure beam are used [41].

3. Validation of the present method

A computer code is developed to determine the critical non-dimensional aerodynamic pressure of the MR sandwich beam using the present formulation. The code is verified using the results of frequency analysis given by [45] letting $\zeta=0$. The dimensions and material properties of the sandwich beam with MR core are taken from Yalcintas and Dai [23]. The obtained results using the present formulation are given in Table 1 beside the results of Yeh and Shih [45], which used the model of Mead and Markus [17] in their formulation. From Table 1 it is seen that the natural frequencies and loss factors obtained by the present method are in good agreement with those of Yeh and Shih, which verifies the validity of the present methodology.

Table 2 shows a comparison of natural frequencies obtained from the present formulation and the results of Nayak et al. [46] for three different boundary conditions which are found to be in good agreement with the results of Nayak et al. [46]. The geometrical and material properties are same as that of examples 1 to 3 of Howson and Zare [47].

4. Results and discussion

Many structure and fluid related parameters such as field intensity, thickness of the fluid layer, geometry of the beam, type of the MR fluid, thicknesses of the elastic face layers, boundary conditions, etc., may influence the aeroelastic behavior of the MR sandwich beam. The proposed assumed mode method is used to study the effect of variations in the constraining and fluid layer thicknesses, magnetic field intensity on the properties of the MR sandwich beam in terms of critical non-dimensional aerodynamic pressure for different boundary conditions.

To show the effectiveness of the constraining damping treatment using MR material to suppress flutter instability, consider an MR sandwich beam with properties specified in Table 3.

In this study the MR fluid, MRF-122EG, is used, which it's complex shear modulus has been reported by Rajamohan et al. [27] as:

$$\begin{aligned}
G'(B)&=-3.3691B^2+4997.5B+0.873\times10^6\ \text{Pa}\\
G''(B)&=-0.9B^2+812.4B+0.1855\times10^6\ \text{Pa}
\end{aligned} \tag{41}$$

where B is the magnetic field intensity in Gauss.

Table 1
Comparison of the first five natural frequencies of the MR sandwich beam.

Mode	Present		Yeh and Shih [45]	
	ω(Hz)	η	ω(Hz)	η
1	19.16	0.00553	19.16	0.00585
2	52.35	0.00531	52.35	0.00561
3	98.38	0.00385	98.38	0.00407
4	159.75	0.00272	159.75	0.00288
5	237.44	0.00197	237.43	0.00208

Table 2
Comparison of the first five natural frequencies of the MR sandwich beam for different boundary conditions.

Boundary condition	Mode number	Natural frequency (Hz)				
		1	2	3	4	5
Clamped–clamped	Present analysis	34.630	93.392	178.049	285.389	410.839
	Nayak et al. [46]	34.669	93.522	178.472	285.810	412.095
	Error (%)	−0.11	−0.14	−0.24	−0.15	−0.31
Simply supported	Present analysis	57.139	219.585	465.171	768.163	1106.626
	Nayak et al. [46]	57.146	223.919	465.932	772.133	1111.1
	Error (%)	−0.01	−1.97	−0.16	−0.52	−0.40
Clamped-free	Present analysis	33.759	199.523	515.399	916.813	1366.679
	Nayak et al. [46]	33.754	199.126	513.174	909.954	1355.30
	Error (%)	0.01	0.20	0.43	0.75	0.83

Table 3
Material properties and geometric parameters of the MR sandwich beam.

Parameters	Value
Length (L)	35 cm
Width (b)	4 cm
Base layer thickness (h_b)	2 mm
Constraining layer thickness (h_c)	1 mm
MR layer thickness (h_f)	2 mm
Base and Constraining layer Young's modulus (E_b, E_c)	70 GPa
Base and Constraining layer density (ρ_b, ρ_c)	2710 kg m^{-3}
MR layer density (ρ_f)	3500 kg m^{-3}

The following non-dimensional parameters are used for parametric study:

$$H_f = h_f/h_b, \quad H_c = h_c/h_b \tag{42}$$

4.1. Aeroelastic analysis

The variation of natural frequencies and loss factors in terms of non-dimensional aerodynamic pressure for MR sandwich beam with S-S, C–C and C-F boundary conditions at 500 Gauss are illustrated in Figs. 3–5. Conventional p-method is used to predict the onset of instability in terms of critical value of non-dimensional aerodynamic pressure (λ_{cr}). Maximum number of eight modes ($N_u = N_w = 8$) guaranties the convergence of λ_{cr} for all of the selected geometric parameters used in this study.

Each figure illustrates the variation of the first five modal frequencies and damping ratios with respect to λ. Aeroelastic instability occurs when, at a specific point, one of the modal loss factors drops below zero. When corresponding modal frequency at the point of instability becomes zero, divergence type instability occurs, while at flutter type instability, corresponding modal frequency is not zero. At flutter instability, above the critical value, two adjacent aeroelastic modes get close to each other but do not merge due to damping of MR layer.

As it can be seen from Figs. 3–5, flutter type instability occurs for S-S and C–C boundary conditions between the first and second modes, while for C-F boundary condition, divergence type instability happens. This has already has been reported by Bisplinghoff and Ashley [48] for clamped-free bare beams in supersonic flow. For all cases considered, the modal damping associated with the first mode crosses the zero axes which indicate that instability boundary has been reached.

4.2. Effect of magnetic field intensity

Fig. 6. indicates variation in λ_{cr} of the MR sandwich beam with S-S, C-F and C–C boundary conditions for different field intensities and different values of constraining layer thickness ratios (H_c). It can be seen that for a specific configuration (say $H_c = 0.5$), the MR sandwich beam with C–C end condition has highest λ_{cr}, while for C-F condition it has the lowest λ_{cr}. This is attributed to the higher stiffness of the beam in the C–C end condition. This condition requires more aerodynamic energy to bring the first and second modes of the beam close to each other. The results show an increase in the λ_{cr} with increase in the magnetic field intensity for all boundary conditions at higher values of H_c (0.5 and 1). A similar trend is reported in [33,34] for electrorheological sandwich

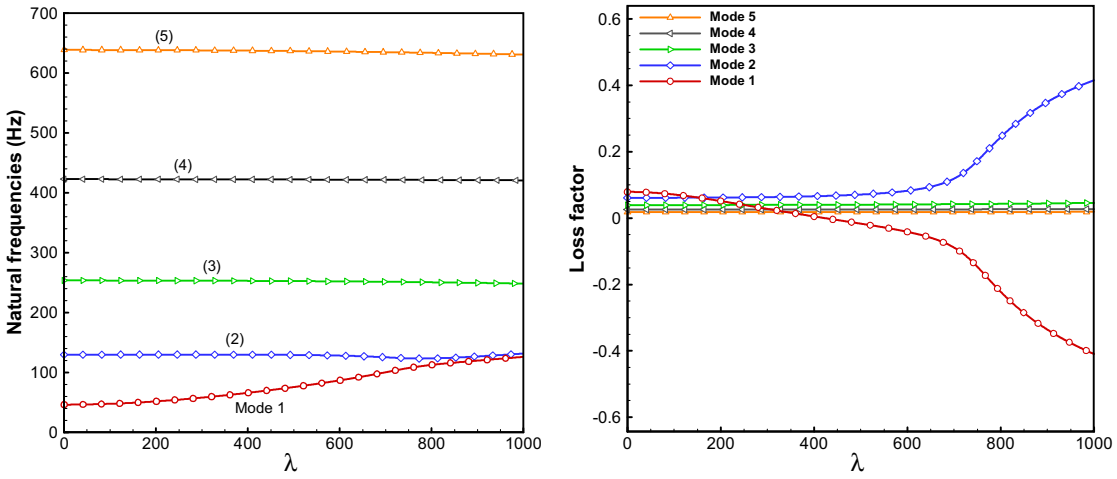

Fig. 3. Natural frequencies and loss factors of simply supported MR sandwich beam varying with non-dimensional aerodynamic pressure at 500 Gauss.

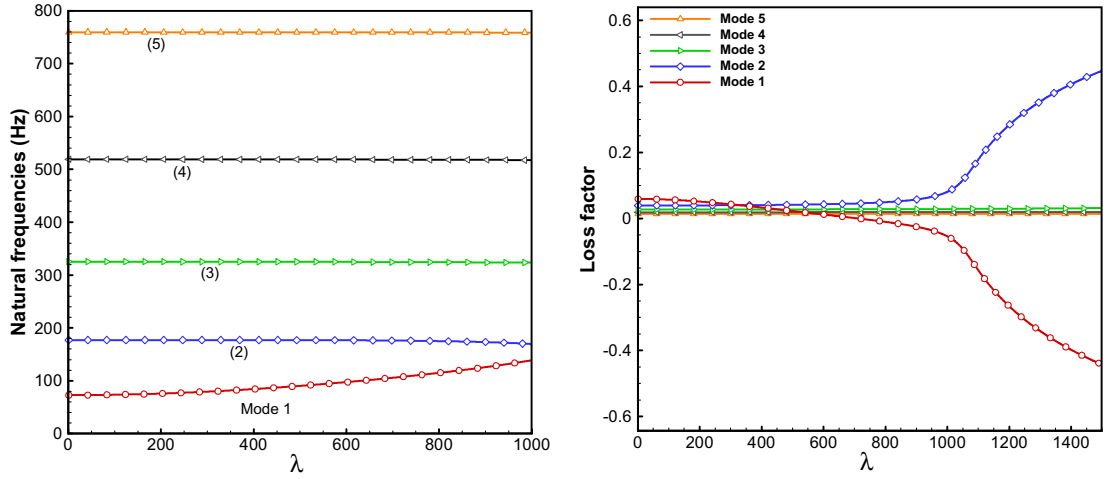

Fig. 4. Natural frequencies and loss factors of clamped–clamped MR sandwich beam varying with non-dimensional aerodynamic pressure at 500 Gauss.

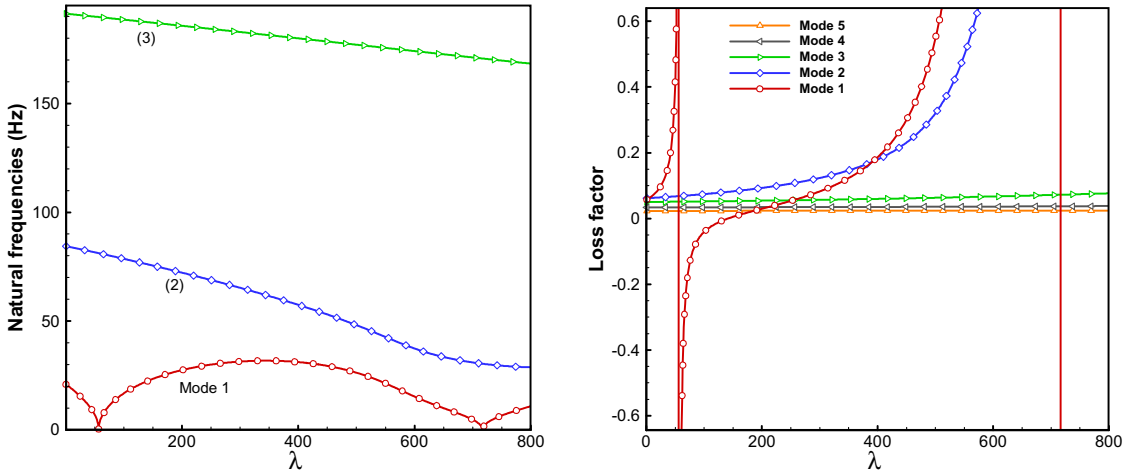

Fig. 5. Natural frequencies and loss factors of clamped-free MR sandwich beam varying with non-dimensional aerodynamic pressure at 500 Gauss.

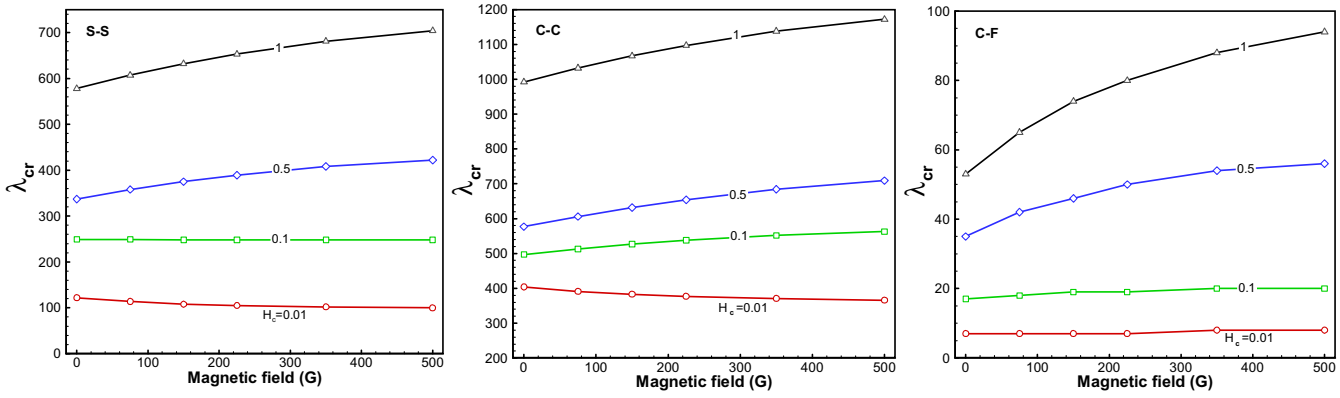

Fig. 6. Influence of magnetic field intensity on λ_{cr} for different values of H_c.

beam and plate. This can be attributed to the fact that with increasing magnetic field intensity, simultaneous upward shift in the first and second mode frequencies occur at high values of H_c. That is to say, modal loss factor of the first mode decreases with increasing magnetic field intensity and has decreasing effect on λ_{cr}. However, this reduction is not so considerable at higher values of thickness ratio. At low values of H_c (0.01 and 0.1), specifically for S-S end condition, there is no obvious upward shift in the first two natural frequencies of the beam. On the other hand, decreasing behavior of the first mode loss factor, shifts λ_{cr} to lower values. To the authors knowledge, this type of behavior has not been reported in the literature.

The effect of magnetic field intensity on λ_{cr} for all three types of boundary conditions for different values of MR layer thickness

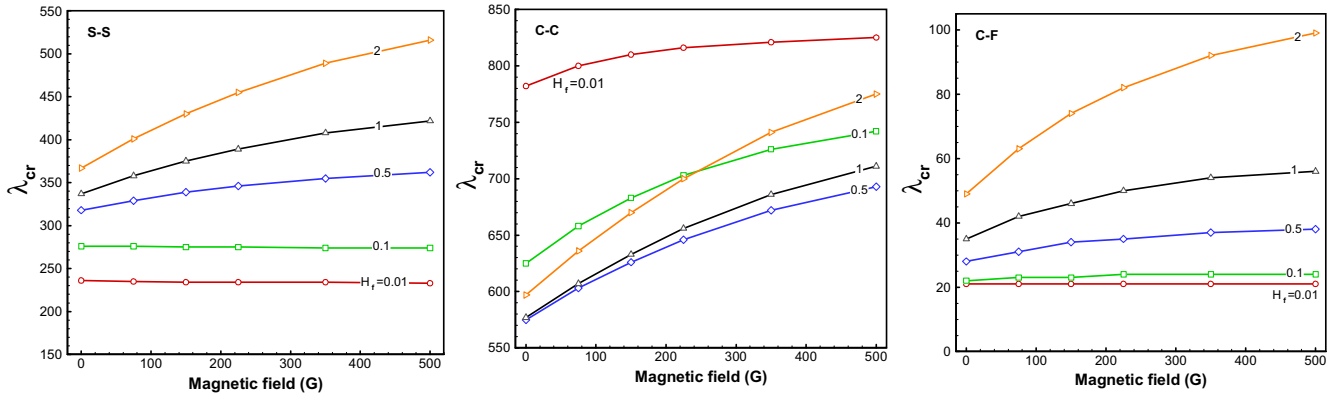

Fig. 7. Influence of the magnetic field intensity on the λ_{cr} for different values of H_f.

ratios (H_f) is illustrated in Fig. 7. For C-F boundary conditions at low values of H_f (0.01 and 0.1) there is a non-significant increase in λ_{cr} and in S-S end condition, a slight decrement is observed. For higher values of H_f (0.5, 1 and 2) the results generally show an increase in λ_{cr} for all three types of boundary conditions.

Furthermore, for C-F and S-S boundary conditions there is an increment in λ_{cr} with increase in the thickness of the MR layer from $H_f = 0.01$ to $H_f = 2$ but for C–C end condition at low values of H_f (0.01 and 0.1) the highest values of λ_{cr} happen. This observation may be related to the role of damping in destabilization of a non-conservative system. According to the works by Dowell, Lottati and Herrmann and Jong [49–51], for lightly damped non-conservative systems adding small structural damping can significantly reduce the instability boundary of the system. The lower the damping, the more reduction in instability boundary. To investigate the effect of damping on the instability boundary of MR sandwich beam, the loss modulus of magneto-rheological fluid is set equal to zero. Table 4 shows variation of λ_{cr} with H_f with and without loss modulus of MR fluid for S-S and C–C boundary conditions corresponding to a fixed field intensity of 0 Gauss. $\omega_1, \eta_1, \omega_2, \eta_2$ indicate first and second mode natural frequencies and loss factors of the beam regardless of aerodynamic pressure. ω_{1f}, ω_{2f} are the frequencies of the first and second mode at fluttering point.

For S-S case, it is observed that the most reduction in instability boundary occurs for lowest value of H_f which has the lowest value of first mode loss factor. With increasing the thickness of the MR layer, the value of the first mode loss factor increases, thus the value of flutter boundary increases. In C–C case, reduction of flutter boundary occurs due to presence of damping, however, lowest value of flutter boundary does not happen at lowest value of H_f. This may be linked to the large values of critical aerodynamic pressure in undamped condition, for low values of H_f (0.01 and 0.1). In addition, for C–C case higher first mode loss factor in comparison with S-S case causes less reduction in critical aerodynamic pressure.

Fig. 8. shows the influence of H_f on the critical aerodynamic pressure at different values of H_c. The magnetic field applied to the MR layer is 500 Gauss.

The results show that in S-S and C-F cases, λ_{cr} increases with increasing the MR layer thickness for all constraining layer thickness values. At lower values of H_c, the similar trend has been observed for C–C case. However, at higher values of H_c, critical

Table 4
Effect of loss modulus of MR fluid on instability boundary.

Boundary condition		H_f	ω_1	ω_2	η_1	η_2	ω_{1f}	ω_{2f}	λ_{cr}
S-S	Damped	0.01	55.22	206.85	0.01059	0.03194	63.22	206.67	237
		0.1	48.39	157.33	0.05592	0.06000	66.02	156.88	277
		0.5	39.05	124.51	0.08775	0.04688	63.96	122.60	318
		1	34.92	109.24	0.10084	0.04850	59.01	107.21	338
		2	31.09	92.95	0.11951	0.05817	52.19	91.27	368
	Undamped	0.01	55.17	206.33	0	0	176.51	176.51	1028
		0.1	48.24	157.10	0	0	136.04	136.04	635
		0.5	38.98	124.4	0	0	105.74	105.74	506
		1	34.88	109.23	0	0	92.87	92.87	505
		2	31.07	92.94	0	0	79.58	79.58	533
C–C	Damped	0.01	116.22	296.20	0.03316	0.04834	149.01	295.53	787
		0.1	88.52	222.60	0.05817	0.04144	128.84	220.40	626
		0.5	70.27	182.34	0.04531	0.02602	106.90	179.37	576
		1	61.65	159.86	0.04685	0.02657	93.95	157.26	578
		2	52.41	134.24	0.05612	0.03248	79.37	132.28	598
		4	43.67	108.96	0.07433	0.04538	65.07	107.84	645
	Undamped	0.01	115.92	295.37	0	0	260.05	260.05	1593
		0.1	88.40	222.47	0	0	194.57	194.57	958
		0.5	70.25	182.32	0	0	157.64	157.64	837
		1	61.64	159.85	0	0	138.25	138.25	837
		2	52.40	134.23	0	0	116.62	116.62	868
		4	43.66	108.96	0	0	95.69	95.69	947

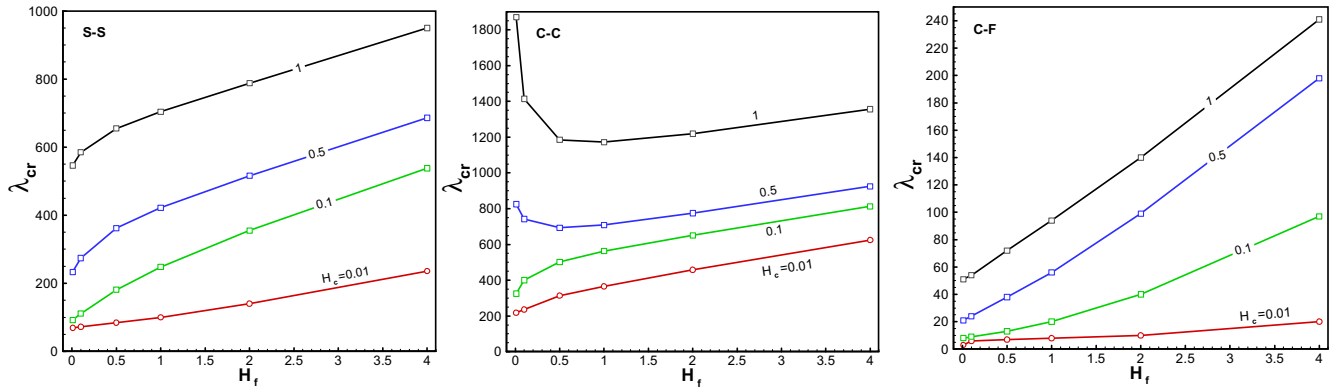

Fig. 8. Influence of variation in H_f on the λ_{cr} corresponding to different H_c at 500 G.

aerodynamic pressure decreases with increasing H_f to 0.5 and then increases monotonically.

5. Conclusion

The aeroelastic characteristics of MR sandwich beams exposed to supersonic airflow are presented. The governing differential equation of motion was derived by utilizing Hamilton's principle. Assumed mode method has been used to solve governing equation of motion along with p-method for aeroelastic instability analysis. Various parametric studies were performed to investigate aeroelastic instability boundary of the MR fluid sandwich beam by the effect of magnetic field intensity, MR layer and constraining layer thicknesses under three frequently encountered boundary conditions. Different types of aeroelastic instability have been discussed for different boundary conditions of the beam. The major outcomes of this study are:

- Flutter type instability occurs for clamped–clamped and simply-supported boundary condition and divergence type instability happens for clamped-free boundary condition.
- For all three types of boundary conditions, increasing the magnetic field intensity will rise the critical non-dimensional aerodynamic pressure for high values of constraining layer thickness; however there is slight reduction or no significant change at lower values of constraining layer thicknesses.
- In simply-supported and clamped-free boundary conditions, the critical aerodynamic pressure increases with increasing magnetic field intensity for different values of MR layer thicknesses. However, clamped–clamped boundary condition has different behavior in comparison with two other boundary conditions, that is, for lower values of MR layer thicknesses the highest critical aerodynamic pressure are observed.
- In simply-supported, clamped-free and lower values of constraining layer thickness in clamped–clamped boundary conditions, at constant magnetic field intensity, increasing the thickness of the MR fluid layer leads to rise in critical aerodynamic pressure for different values of constraining layer thicknesses. There is an exception for clamped–clamped boundary condition at higher values of constraining layer thicknesses which drops with increasing the thickness of the MR layer to 0.5 and then rises monotonically.

References

[1] Song Z-G, Li F-M. Active aeroelastic flutter analysis and vibration control of supersonic beams using the piezoelectric actuator/sensor pairs. Smart Mater Struct 2011;20:055013.
[2] Singha MK, Mandal M. Supersonic flutter characteristics of composite cylindrical panels. Compos Struct 2008;82:295–301.
[3] Kouchakzadeh MA, Rasekh M, Haddadpour H. Panel flutter analysis of general laminated composite plates. Compos Struct 2010;92:2906–15.
[4] Zhao H, Cao D. A study on the aero-elastic flutter of stiffened laminated composite panel in the supersonic flow. J Sound Vib 2013;332:4668–79.
[5] Li F-M, Song Z-G. Flutter and thermal buckling control for composite laminated panels in supersonic flow. J Sound Vib 2013;332:5678–95.
[6] Kerboua M, Megnounif A, Benguediab M, Benrahou KH, Kaoulala F. Vibration control beam using piezoelectric-based smart materials. Compos Struct 2015;123:430–42.
[7] Daghia F, Inman DJ, Ubertini F, Viola E. Shape memory alloy hybrid composite plates for shape and stiffness control. J Intell Mater Syst Struct 2008;19:609–19.
[8] Hasheminejad SM, Maleki M. Free vibration and forced harmonic response of an electrorheological fluid-filled sandwich plate. Smart Mater Struct 2009;18:055013.
[9] Lara-Prieto V, Parkin R, Jackson M, Silberschmidt V, Kęsy Z. Vibration characteristics of MR cantilever sandwich beams: experimental study. Smart Mater Struct 2010;19:015005.
[10] Ramamoorthy M, Rajamohan V, AK J. Vibration analysis of a partially treated laminated composite magnetorheological fluid sandwich plate. J Vib Control 2016;22:869–95.
[11] Manoharan R, Vasudevan R, Jeevanantham AK. Dynamic characterization of a laminated composite magnetorheological fluid sandwich plate. Smart Mater Struct 2014;23:025022.
[12] Rajamohan V, Sedaghati R, Rakheja S. Optimal vibration control of beams with total and partial MR-fluid treatments. Smart Mater Struct 2011;20:115016.
[13] Hoseinzadeh M, Rezaeepazhand J. Vibration suppression of composite plates using smart electrorheological dampers. Int J Mech Sci 2014;84:31–40.
[14] Tabassian R, Rezaeepazhand J. Dynamic stability of smart sandwich beams with electro-rheological core resting on elastic foundation. J Sandwich Struct Mater 2013;15:25–44.
[15] Gandhi MV, Thompson BS, Choi SB. A new generation of innovative ultra-advanced intelligent composite materials featuring electro-rheological fluids: an experimental investigation. J Compos Mater 1989;23:1232–55.
[16] Haiqing G, King Lim Mong, Cher Tan Bee. Influence of a locally applied electro-rheological fluid layer on vibration of a simple cantilever beam. J Intell Mater Syst Struct 1993;4:379–84.
[17] Mead DJ, Markus S. The forced vibration of a three-layer, damped sandwich beam with arbitrary boundary conditions. J Sound Vib 1969;10:163–75.
[18] Yalcintas M, Coulter JP. An adaptive beam model with electrorheological material based applications. J Intell Mater Syst Struct 1995;6:498–507.
[19] Allahverdizadeh A, Eshraghi I, Mahjoob MJ, Nasrollahzadeh N. Nonlinear vibration analysis of FGER sandwich beams. Int J Mech Sci 2014;78:167–76.
[20] Allahverdizadeh A, Mahjoob MJ, Nasrollahzadeh N, Eshraghi I. Optimal parameters estimation and vibration control of a viscoelastic adaptive sandwich beam incorporating an electrorheological fluid layer. J Vib Control 2014;20:1855–68.
[21] Allahverdizadeh A, Mahjoob MJ, Maleki M, Nasrollahzadeh N, Naei MH. Structural modeling, vibration analysis and optimal viscoelastic layer characterization of adaptive sandwich beams with electrorheological fluid core. Mech Res Commun 2013;51:15–22.
[22] Allahverdizadeh A, Mahjoob MJ, Eshraghi I, Nasrollahzadeh N. On the vibration behavior of functionally graded electrorheological sandwich beams. Int J Mech Sci 2013;70:130–9.
[23] Yalcintas M, Dai H. Magnetorheological and electrorheological materials in adaptive structures and their performance comparison. Smart Mater Struct 1999;8:560.
[24] Sun Q, Zhou J-X, Zhang L. An adaptive beam model and dynamic characteristics of magnetorheological materials. J Sound Vib 2003;261:465–81.
[25] Yeh Z-F, Shih Y-S. Dynamic characteristics and dynamic instability of magnetorheological material-based adaptive beams. J Compos Mater 2006;40:1333–59.

[26] Ganesan N, Ramkumar K. Vibration and damping studies on a hollow sandwich box column with a viscoelastic/electrorheological/magnetorheological fluid core layer by the finite element method. Int J Struct Stab Dyn 2008;8:531–46.
[27] Rajamohan V, Sedaghati R, Rakheja S. Vibration analysis of a multi-layer beam containing magnetorheological fluid. Smart Mater Struct 2010;19:015013.
[28] Choi Y, Sprecher A, Conrad H. Vibration characteristics of a composite beam containing an electrorheological fluid. J Intell Mater Syst Struct 1990;1:91–104.
[29] Rajamohan V, Rakheja S, Sedaghati R. Vibration analysis of a partially treated multi-layer beam with magnetorheological fluid. J Sound Vib 2010;329:3451–69.
[30] Rajamohan V, Sedaghati R, Rakheja S. Optimum design of a multilayer beam partially treated with magnetorheological fluid. Smart Mater Struct 2010;19:065002.
[31] Ying ZG, Ni YQ, Ye SQ. Stochastic micro-vibration suppression of a sandwich plate using a magneto-rheological visco-elastomer core. Smart Mater Struct 2014;23:025019.
[32] Eshaghi M, Sedaghati R, Rakheja S. The effect of magneto-rheological fluid on vibration suppression capability of adaptive sandwich plates: experimental and finite element analysis. J Intell Mater Syst Struct 2015;26:1920–35.
[33] Hasheminejad SM, Nezami M, Panah MEA. Supersonic flutter suppression of electrorheological fluid-based adaptive panels resting on elastic foundations using sliding mode control. Smart Mater Struct 2012;21:045005.
[34] Rahiminasab J, Rezaeepazhand J. Aeroelastic stability of smart sandwich plates with electrorheological fluid core and orthotropic faces. J Intell Mater Syst Struct 2013;24:669–77.
[35] Aryaeepanah ME, Hasheminejad SM, Nezami M. Flutter suppression of an elastically supported plate with electro-rheological fluid core under yawed supersonic flows. Int J Struct Stab Dyn 2013;13:1250073.
[36] Motaaleghi MA, Hasheminejad SM. Supersonic flutter control of an electrorheological fluid-based smart circular cylindrical shell. Int J Struct Stab Dyn 2014;14:1350064.
[37] Hasheminejad SM, Aghayi Motaaleghi M. Aeroelastic analysis and active flutter suppression of an electro-rheological sandwich cylindrical panel under yawed supersonic flow. Aerosp Sci Technol 2015;42:118–27.
[38] Reddy JN. Theory and Analysis of Elastic Plates and Shells. Taylo & Francis; 2006.
[39] Li WH, Chen G, Yeo SH. Viscoelastic properties of MR fluids. Smart Mater Struct 1999;8:460.
[40] Choi YT, Cho JU, Choi SB, Wereley NM. Constitutive models of electrorheological and magnetorheological fluids using viscometers. Smart Mater Struct 2005;14:1025.
[41] Rao SS. Vibration of Continuous Systems. John Wiley & Sons; 2007.
[42] Shin W-H, Oh I-K, Han J-H, Lee I. Aeroelastic characteristics of cylindrical hybrid composite panels with viscoelastic damping treatments. J Sound Vib 2006;296:99–116.
[43] Koo K-N, Hwang W-S. Effects of hysteretic and aerodynamic damping on supersonic panel flutter of composite plates. J Sound Vib 2004;273:569–83.
[44] Li F-M, Chen Z-B, Cao D-Q. Improving the aeroelastic flutter characteristics of supersonic beams using piezoelectric material. J Intell Mater Syst Struct 2011;22:615–29.
[45] Yeh Z-F, Shih Y-S. Dynamic stability of a sandwich beam with magnetorheological core. Mech Based Des. Struct. Mach. 2006;34:181–200.
[46] Nayak B, Dwivedy SK, Murthy KSRK. Dynamic stability of magnetorheological elastomer based adaptive sandwich beam with conductive skins using FEM and the harmonic balance method. Int J Mech Sci 2013;77:205–16.
[47] Howson WP, Zare A. Exact dynamic stiffness matrix for flexural vibration of three-layered sandwich beams. J Sound Vib 2005;282:753–67.
[48] Bisplinghoff RL, Ashley H. Principles of Aeroelasticity. Dover Publications; 2002.
[49] Dowell EH. Panel flutter – a review of the aeroelastic stability of plates and shells. AIAA J. 1970;8:385–99.
[50] Lottati I. The role of damping on supersonic panel flutter. AIAA J. 1985;23:1640–2.
[51] Herrmann G, Jong I-C. On the destabilizing effect of damping in nonconservative elastic systems. J Appl Mech 1965;32:592–7.